JACS
JOURNAL OF THE AMERICAN CHEMICAL SOCIETY
Communication
pubs.acs.org/JACS

Environmentally Benign Synthesis of Ultrathin Metal Telluride Nanowires

Haoran Yang,[†] Scott W. Finefrock,[†] Jonatan D. Albarracin Caballero, and Yue Wu[‡,*]

School of Chemical Engineering, Purdue University, West Lafayette, Indiana 47907, United States

Supporting Information

ABSTRACT: Metal telluride nanowires are attractive materials for many applications, yet most synthesis recipes require hazardous reducing agents such as hydrazine or sodium borohydride. We describe a two-step synthesis of various metal tellurides with nanowire morphology using a nonhazardous reducing agent, ascorbic acid. In the first step, Te grows one-dimensionally to form ultrathin nanowires; in the second step, these nanowires are converted to metal telluride nanowires by adding metal precursors. Analysis of the reaction products versus time provides insights into the growth and conversion mechanisms as well as the reaction rates.

Metal tellurides are important materials in the areas of thermoelectrics,[1,2] photovoltaics,[3] radiation detection,[4] and others.[5,6] Nanowires and nanowire-based composites of these and other materials possess unique properties compared to bulk materials; for example, reduced thermal conductivity and altered electron scattering[7,8] as well as enhanced light absorption[9] and compatibility with flexible substrates.[10] Nanowires synthesized by solution-based approaches have the additional potential advantage of low-cost manufacturing for large-scale applications.

Among the published methods for solution synthesis of metal telluride nanowires, many require the reducing agent, hydrazine, which is extremely hazardous.[11−17] Even alterative reducing agents such as hydroxylamine[18] and sodium borohydride[19−21] are still moderately hazardous or highly flammable. Meanwhile, ascorbic acid (vitamin C) is a relatively safe reducing agent that has been used in many solution-based syntheses of inorganic materials[22−27] including Te nanowires.[28−30] In a few cases, ascorbic acid has been used to synthesize metal telluride nanowires, yet prior synthesis methods have resulted in nanowires with several nanometer thick carbonaceous sheaths[31,32] or poor control over the nanostructure morphology when synthesizing a broad range of metal tellurides.[33]

Here, we show how dissolved Te precursor can not only be reduced to form nanowires using ascorbic acid, but also how these Te nanowire can be converted into a variety of metal telluride nanowires including PbTe, CdTe, Bi_2Te_3, Ag_2Te, and $Cu_{1.75}Te$. A schematic of this general one-pot synthesis strategy is shown in Figure 1a.

The synthesis of Te nanowires is accomplished as follows: TeO_2, polyvinylpyrrolidone (PVP), and KOH are dissolved in ethylene glycol (EG) resulting in a cloudy white solution. The temperature is raised to 120 °C, causing the solution to become transparent yellow. Then an aqueous solution of ascorbic acid is rapidly added, which results in a change in color to opaque black within about 2 min. This first reaction step then proceeds for 24 h. For the conversion to PbTe, CdTe, or Bi_2Te_3, the appropriate metal cation and PVP are dissolved in EG. This metal cation precursor solution is added to the Te reaction mixture along with additional aqueous ascorbic acid. This second reaction step proceeds for 24 h after which the mixture is cooled to room temperature and washed with deionized water.

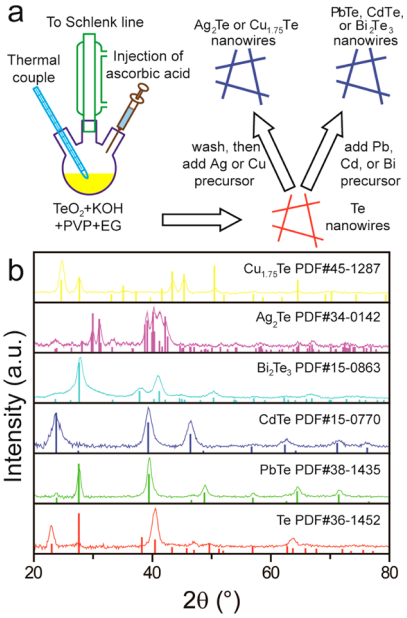

Figure 1. (a) Metal telluride nanowire synthesis strategy. (b) XRD patterns of Te and metal telluride synthesis products.

Conversion to Ag_2Te or $Cu_{1.75}Te$ requires an approach similar to that which was developed by Shu-Hong Yu's group.[34] After the 24 h synthesis of Te, the reaction mixture is cooled to room temperature and washed several times with water to remove unreacted ascorbic acid and KOH. The obtained solid Te is dissolved in EG at room temperature, and a solution of silver or copper precursor in EG is added slowly. The reaction proceeds at room temperature for 1 h after which the products are washed with deionized water.

Received: May 27, 2014
Published: July 8, 2014

   dx.doi.org/10.1021/ja505304v | J. Am. Chem. Soc. 2014, 136, 10242−10245

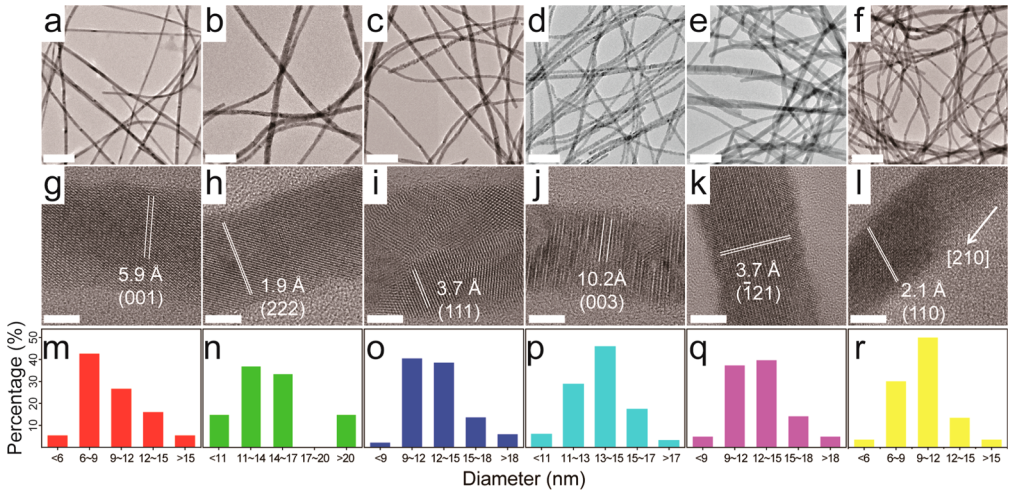

Figure 2. TEM analysis of nanowire materials synthesized using ascorbic acid. (a–f) Low-magnification TEM, scale bars represent 100 nm. (g–l) HRTEM, scale bars represent 5 nm. (m–r) Histograms of diameters. The six columns correspond to the six materials synthesized: (a,g,m) Te; (b,h,n) PbTe; (c,i,o) CdTe; (d,j,p) Bi_2Te_3; (e,k,q) Ag_2Te; (f,l,r) $Cu_{1.75}Te$.

X-ray diffraction (XRD) patterns of the synthesis products are shown in Figure 1b. The pattern for the Te synthesized in the first step corresponds well to that of trigonal Te except that peaks from planes such as (001) are diminished or absent. This suggests that the (001) planes of the crystals are preferentially aligned perpendicularly to the surface of the substrate used during XRD. Such substrate-induced alignment has been observed in several other nanowire materials.[35−38] Furthermore, all peaks present are quite broad indicating a small crystal size. Both of these observations agree with the transmission electron microscopy (TEM) analysis, described later, which reveals ultrathin Te nanowires with *c*-axes perpendicular to the substrate. The XRD patterns of the metal telluride products of the second reaction step can all be indexed to the corresponding patterns from the literature. In all cases, broad peaks are observed in accordance with small grain sizes.

TEM analysis of all six materials is shown in Figure 2. The low-magnification TEM image and high-resolution TEM (HRTEM) image of Te (Figure 2a,g) reveal nanowire morphology with an axial direction aligned with the [001] direction of Te. The nanowire morphology is due to the anisotropic crystal structure of Te[11,39] as well as the presence of PVP as a structure directing agent.[40,41] Low-magnification TEM images (Figure 2b–f) of PbTe, CdTe, Bi_2Te_3, Ag_2Te, and $Cu_{1.75}Te$ synthesis products reveal that all possess nanowire morphology, thus illustrating that in the second reaction step, the Te nanowires are then converted into metal telluride nanowires while preserving the original nanowire morphology.

The HRTEM image of a typical PbTe nanowire (Figure 2h) shows a single crystalline region in which the nanowire axis is aligned with the [222] crystal direction. Additionally, a small fraction of PbTe nanowires showed regions with axial directions aligned with the [220] crystal direction (Figure S1). This is similar to our previous results for PbTe nanowires synthesized using Te nanowire templates, which showed both [222] and [220] axial directions[42] and is different from the [200] axial direction observed in PbTe nanowires grown using two-step hydrothermal methods.[17,31] Figure 2i shows a typical CdTe nanowire; it is polycrystalline with numerous small grains, yet the fast Fourier transform (Figure S2) indicates diffraction spots that can be indexed as zinc-blende CdTe with a few spots from wurtzite CdTe. Thus, while XRD indicates that the majority of CdTe is in the zinc-blende phase, a small amount takes the wurtzite phase. Some solution syntheses can yield single crystalline zinc-blende CdTe nanowires,[18,31,43] yet the presence of defects is fairly common for CdTe nanowire synthesized in solution,[14,44] and it is common for both wurtzite and zinc blende phases to be observed within single nanowires.[10,18,37] In the case of Bi_2Te_3, the HRTEM image (Figure 2j) shows a single crystalline region with an axial direction aligned with the [003] crystal direction as observed in other solution-synthesized 1D Bi_2Te_3.[42,45,46] Among the various metal telluride nanowires, Ag_2Te nanowires are unique in that there is not a single crystalline direction that consistently aligns with the nanowire axis even within the same batch. While the nanowire presented in Figure 2k shows an axial direction of [$\bar{1}$21], this differs for other Ag_2Te nanowires analyzed (Figure S3). Solution-synthesized Ag_2Te nanowires and nanorods described in literature also follow this trend.[18,47−50] Finally, the HRTEM image of a typical $Cu_{1.75}Te$ nanowire reveals a large single crystalline region with an axial direction of [210], unlike $Cu_{2-x}Te$ nanowires described in literature.[51,52]

For each material, the diameters of more than 25 nanowires were measured. The diameter distributions shown in Figure 2m–r show that the original Te nanowires have diameters of 9.7 ± 2.7 nm and the metal telluride nanowires have average diameters in the range of 10.0–14.6 nm. Thus, the diameters increase slightly due to metal addition during the second reaction step.

To better understand the Te nanowire formation mechanism as well as the reaction rate achieved using ascorbic acid, experiments are performed to observe the reaction products over time during the Te nanowire growth step. Aliquots are taken from the reactions by collecting 1–2 mL and quenching in water. The material is washed two times with water, dispersed in ethanol, and drop cast onto TEM grids. Aliquot samples are obtained 5 min, 20 min, 1.5, 3.5, 7.25, and 24 h after ascorbic acid addition. As the reaction mixture very gradually changes from transparent to opaque within 2 min, it is not surprising that the product in the aliquot taken at 5 min is too dilute to observe any solids after centrifuging. Figure 3a–e shows TEM images of the products obtained from the remaining 5 aliquots. As seen in Figure 3a, the nanowires begin as short nanorods with small diameters. As the reaction

dx.doi.org/10.1021/ja505304v | J. Am. Chem. Soc. 2014, 136, 10242−10245

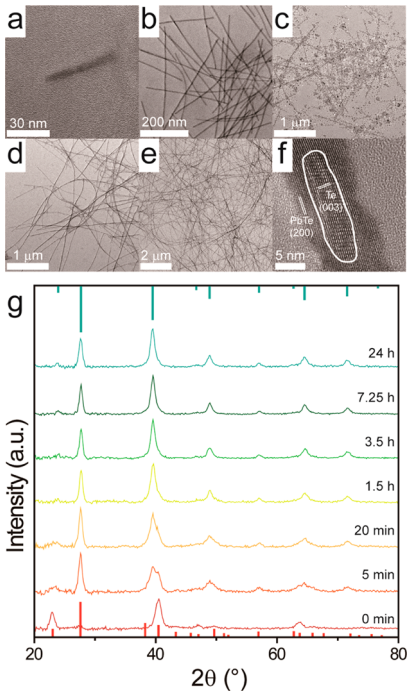

Figure 3. (a–e) TEM images of aliquots taken at various times during the Te nanowire synthesis step: (a) 20 min; (b) 1.5 h; (c) 3.5 h; (d) 7.25 h; (e) 24 h. (f) TEM image of aliquot taken 5 min after Pb precursor injection. (g) XRD patterns of aliquots taken at various times during the conversion from Te nanowires to PbTe nanowires.

continues, the nanowire diameter stays approximately constant, while the length increases almost linearly with time up to greater than 7 μm after 24 h. The spherical particles observed at 3.5 h are likely amorphous tellurium, which is later absorbed into the crystalline nanowires through the ripening process as described in literature and as suggested by their absence from the products obtained after 24 h.[53,54]

The slow growth of Te nanowires induced by ascorbic acid observed here agrees with the long growth times (≥12 h) employed in several hydrothermal and other solution-phase syntheses of Te nanowires using ascorbic acid[28,29,31] or other weak reducing agents such as starch,[55] PVP,[40] EG,[39] or alginic acid.[56] Conversely, solution synthesis of Te nanowires under similar conditions occurs within 1 h or less when hydrazine is used as the reducing agent.[12,42,57,58] This highlights the relatively high strength of hydrazine as a reducing agent as compared with ascorbic acid. That similar products can be produced using reducing agents with such different strengths is an interesting phenomenon which requires further investigation to better comprehend.

We perform similar aliquot studies during the second reaction step to observe the transformation from tellurium to metal tellurides. As an example, the transformation to PbTe is presented in Figure 3g. XRD patterns obtained from reactions products immediately prior to Pb precursor addition as well as 5 min, 20 min, 1.5, 3.5, 7.25, and 24 h after Pb precursor addition are shown in order from bottom to top. The diffraction peaks for PbTe appear after only 5 min, yet a shoulder from the Te peak at 40.5° is present even after 1.5 h and is essentially absent after the conversion reaction proceeds for 3.5 h. Therefore, like the Te growth step, the conversion to PbTe when using ascorbic acid is much slower than when using hydrazine.[42,58]

The conversion from Te to PbTe is further elucidated by Figure 3f, which shows a HRTEM image of a nanowire from the aliquot taken 5 min after Pb precursor addition. Lattice fringes with a spacing of ~0.59 nm, consistent with the (001) planes of Te, are present only in the central portion of the nanowire, while lattice fringes associated with PbTe are mainly present on the nanowire surface. This suggests that Pb atoms are incorporated into the Te nanowire radially from the outside to the inside instead of axially beginning from the nanowire ends. Such a mechanism for the conversion from Te nanowires to metal telluride nanowires has been suggested in several previous reports,[14,17,31,33] yet to our knowledge, ours is the first work to observe such a mechanism by HRTEM.

Results from aliquot studies of the conversions to CdTe, Bi_2Te_3, Ag_2Te, and $Cu_{1.75}Te$ are given in Figure S4. The XRD patterns from aliquots taken at various times suggest that the conversion to CdTe requires only 5 min, which is much less than the amount of time allotted during hydrothermal syntheses, even those which employ hydrazine.[14,31,33] Full conversion to Bi_2Te_3 requires 1.5 h, which is longer than the conversion step in similar syntheses using hydrazine.[12,13,42] As described above, the conversion to Ag_2Te and $Cu_{1.75}Te$ requires less time and lower temperature as compared with conversation to other metal tellurides. The XRD patterns in Figures S4c and S4d show that full conversion is achieved within 5 and 15 min for Ag_2Te and $Cu_{1.75}Te$, respectively, highlighting the rapid diffusion of Ag and Cu ions into Te nanowires.[18,52,59]

The yield of each metal telluride nanowire synthesis was calculated based on the mass of starting precursors and the mass of the washed and dried reaction products. For PbTe, CdTe, and Bi_2Te_3 the yields were approximately 83.3%, 87.5%, and 77.3%, respectively, which points to the feasibility of large-scale synthesis of these materials. For Ag_2Te and $Cu_{1.75}Te$, the yields were about 24.5% and 58.9%, respectively, which is lower likely due to the loss of product while washing Te nanowires prior to metal precursor addition.

In summary, the two-step Te nanowire self-templated synthesis methods presented here produce pure-phase ultrathin metal telluride nanowires as shown by XRD and TEM. The reactions proceed through the use of the environmentally benign reducing reagent, ascorbic acid. The tellurium growth step requires 24 h, while the conversion to metal tellurides requires 3.5 h or less. Finally, reaction yields of >75% are achieved during the synthesis of PbTe, CdTe, and Bi_2Te_3.

■ ASSOCIATED CONTENT

Ⓢ Supporting Information

Experimental details for the synthesis of all five metal telluride nanowires. Additional HRTEM images of PbTe and Ag_2Te. FFT of HRTEM of CdTe. XRD patterns of aliquots taken during the conversion to CdTe, Bi_2Te_3, Ag_2Te, and $Cu_{1.75}Te$. This material is available free of charge via the Internet at http://pubs.acs.org.

■ AUTHOR INFORMATION

Corresponding Author

yuewu@iastate.edu

Present Address

‡Department of Chemical and Biological Engineering, Iowa State University, 2033 Sweeney Hall, Ames, IA 50010.

Author Contributions

[†]These authors contributed equally.

Notes

The authors declare no competing financial interest.

■ ACKNOWLEDGMENTS

S.W.F. thanks Xiaoqin Zhu for assistance with data analysis. This work is supported by US Air Force Office of Scientific Research (award no. FA9550-12-1-0061).

■ REFERENCES

(1) Gaultois, M. W.; Sparks, T. D.; Borg, C. K. H.; Seshadri, R.; Bonificio, W. D.; Clarke, D. R. *Chem. Mater.* **2013**, *25*, 2911.
(2) Sootsman, J. R.; Chung, D. Y.; Kanatzidis, M. G. *Angew. Chem., Int. Ed. Engl.* **2009**, *48*, 8616.
(3) Zweibel, K. *Sol. Energy Mater. Sol. C* **2000**, *63*, 375.
(4) Yang, G.; James, R. B. In *CdTe and Related Compounds; Physics, Defects, Hetero- and Nano-structures, Crystal Growth, Surfaces and Applications: Part II: Crystal Growth, Surfaces and Applications*; Triboulet, R.; Siffert, P., Eds.; Elsevier: Amsterdam, The Netherlands, 2010; pp 214−238.
(5) Ravich, Y. I.; Efimova, B. A.; Smirnov, I. A. *Semiconducting Lead Chalcogenides*; Plenum Press: New York, 1970.
(6) Kudryavtsev, A. A. *The Chemistry and Technology of Selenium and Tellurium*; Collet's LTD: London and Wellingbrough, 1974.
(7) Qiu, B.; Bao, H.; Zhang, G.; Wu, Y.; Ruan, X. *Comput. Mater. Sci.* **2012**, *53*, 278.
(8) Qi, Y.; Wang, Z.; Zhang, M.; Yang, F.; Wang, X. *J. Mater. Chem. A* **2013**, *1*, 6110.
(9) Krogstrup, P.; Jørgensen, H.; Heiss, M.; Jørgensen, H. I.; Demichel, O.; Holm, J. V.; Aagesen, M.; Nygard, J.; Morral, A. F. i. *Nat. Photonics* **2013**, *7*, 306.
(10) Hou, T.-C.; Yang, Y.; Lin, Z.-H.; Ding, Y.; Park, C.; Pradel, K. C.; Chen, L.-J.; Lin Wang, Z. *Nano Energy* **2013**, *2*, 387.
(11) Liang, H.; Liu, J.; Qian, H.; Yu, S. *Acc. Chem. Res.* **2013**, *46*, 1450.
(12) Zhang, G.; Kirk, B.; Jauregui, L. a; Yang, H.; Xu, X.; Chen, Y. P.; Wu, Y. *Nano Lett.* **2011**, *12*, 56.
(13) Wang, K.; Liang, H.-W.; Yao, W.-T.; Yu, S.-H. *J. Mater. Chem.* **2011**, *21*, 15057.
(14) Liang, H.-W.; Liu, S.; Wu, Q.-S.; Yu, S.-H. *Inorg. Chem.* **2009**, *48*, 4927.
(15) Mu, L.; Wan, J.; Ma, D.; Zhang, R.; Yu, W.; Qian, Y. *Chem. Lett.* **2005**, *34*, 52.
(16) Tai, G.; Guo, W.; Zhang, Z. *Cryst. Growth Des.* **2008**, *8*, 2906.
(17) Tai, G.; Zhou, B.; Guo, W. *J. Phys. Chem. C* **2008**, *112*, 11314.
(18) Moon, G. D.; Ko, S.; Xia, Y.; Jeong, U. *ACS Nano* **2010**, *4*, 2307.
(19) Paul, B.; V, A. K.; Banerji, P. *J. Appl. Phys.* **2010**, *108*, 064322.
(20) Kim, C.; Kim, D. H.; Kim, H.; Chung, J. S. *ACS Appl. Mater. Interfaces* **2012**, *4*, 2949.
(21) Ramasamy, K.; Nejo, A. O.; Ziqubu, N.; Rajasekhar, P. V. S. R.; Nejo, A. A.; Revaprasadu, N.; O'Brien, P. *Eur. J. Inorg. Chem.* **2011**, *2011*, 5196.
(22) Jana, N.; Gearheart, L.; Murphy, C. *J. Phys. Chem. B* **2001**, *105*, 4065.
(23) Jana, N. R.; Gearheart, L.; Murphy, C. J. *Chem. Commun.* **2001**, 617.
(24) Jana, N.; Gearheart, L.; Murphy, C. *Adv. Mater.* **2001**, *13*, 1389.
(25) Magdassi, S.; Grouchko, M.; Berezin, O.; Kamyshny, A. *ACS Nano* **2010**, *4*, 1943.
(26) Senthil kumaran, C. K.; Agilan, S.; Velauthapillai, D.; Muthukumarasamy, N.; Thambidurai, M.; Senthil, T. S.; Balasundaraprabhu, R. *ISRN Nanotechnol.* **2011**, *2011*, 589073.
(27) Li, Q.; Yam, V. W.-W. *Chem. Commun.* **2006**, *1*, 1006.
(28) Xi, G.; Liu, Y.; Wang, X.; Liu, X.; Peng, Y.; Qian, Y. *Cryst. Growth Des.* **2006**, *6*, 2567.
(29) Yang, L.; Chen, Z.-G.; Han, G.; Cheng, L.; Xu, H.; Zou, J. *Cryst. Growth Des.* **2013**, *13*, 4796.
(30) See, K. C.; Feser, J. P.; Chen, C. E.; Majumdar, A.; Urban, J. J.; Segalman, R. A. *Nano Lett.* **2010**, *10*, 4664.
(31) Xi, G.; Wang, C.; Wang, X.; Qian, Y.; Xiao, H. *J. Phys. Chem. C* **2008**, *112*, 965.
(32) Yong, S.; Muralidharan, P.; Kim, D.; Kim, D. *Rev. Adv. Mater. Sci.* **2011**, *28*, 13.
(33) Jiang, L.; Zhu, Y.-J.; Cui, J.-B. *Eur. J. Inorg. Chem.* **2010**, *2010*, 3005.
(34) Liu, J.-W.; Xu, J.; Liang, H.-W.; Wang, K.; Yu, S.-H. *Angew. Chem., Int. Ed. Engl.* **2012**, *51*, 7420.
(35) Grebinski, J.; Hull, K.; Zhang, J. *Chem. Mater.* **2004**, *16*, 5260.
(36) Hull, K.; Grebinski, J.; Kosel, T.; Kuno, M. *Chem. Mater.* **2005**, *17*, 4416.
(37) Kuno, M.; Ahmad, O.; Protasenko, V.; Bacinello, D.; Kosel, T. H. *Chem. Mater.* **2006**, *18*, 5722.
(38) Jiang, F.; Liu, J.; Li, Y.; Fan, L. *Adv. Funct. Mater.* **2012**, *22*, 2402.
(39) Song, J. M.; Lin, Y. Z.; Zhan, Y. J.; Tian, Y. C.; Liu, G.; Yu, S. *Cryst. Growth Des.* **2008**, *8*, 1902.
(40) Zhu, Y.-J.; Hu, X.-L.; Wang, W.-W. *Nanotechnology* **2006**, *17*, 645.
(41) Qiang, H.-S.; Yu, S.-H.; Gong, J.-Y.; Luo, L.-B.; Fei, L. *Langmuir* **2006**, *22*, 3830.
(42) Finefrock, S. W.; Fang, H.; Yang, H.; Darsono, H.; Wu, Y. *Nanoscale* **2014**, *6*, 7872.
(43) Gong, H.; Hao, X.; Gao, C.; Wu, Y.; Du, J.; Xu, X.; Jiang, M. *Nanotechnology* **2008**, *19*, 445603.
(44) Tang, Z.; Kotov, N. a; Giersig, M. *Science.* **2002**, *297*, 237.
(45) Yu, H.; Gibbons, P.; Buhro, W. *J. Mater. Chem.* **2004**, *14*, 595.
(46) Zhu, H.-T.; Luo, J.; Fan, H.-M.; Zhang, H.; Liang, J.-K.; Rao, G.-H.; Li, J.-B.; Liu, G.-Y.; Du, Z.-M. *J. Mater. Chem.* **2011**, *21*, 12375.
(47) Zhang, L.; Yu, J. C.; Mo, M.; Wu, L.; Kwong, K. W.; Li, Q. *Small* **2005**, *1*, 349.
(48) Qin, A.; Fang, Y.; Tao, P.; Zhang, J.; Su, C. *Inorg. Chem.* **2007**, *46*, 7403.
(49) Samal, A. K.; Pradeep, T. *J. Phys. Chem. C* **2009**, *113*, 13539.
(50) Li, N.; Zhao, B.; Zhou, S.; Lou, S.; Wang, Y. *Mater. Lett.* **2012**, *81*, 212.
(51) Wan, B.; Hu, C.; Zhou, W.; Liu, H.; Zhang, Y. *Solid State Sci.* **2011**, *13*, 1858.
(52) Dong, G.-H.; Zhu, Y.-J.; Cheng, G.-F.; Ruan, Y.-J. *Mater. Lett.* **2012**, *76*, 69.
(53) Gautam, U. K.; Rao, C. N. R. *J. Mater. Chem.* **2004**, *14*, 2530.
(54) Tao, H.; Shan, X.; Yu, D.; Liu, H.; Qin, D.; Cao, Y. *Nanoscale Res. Lett.* **2009**, *4*, 963.
(55) Lu, Q.; Gao, F.; Komarneni, S. *Langmuir* **2005**, *21*, 6002.
(56) Lu, Q.; Gao, F.; Komarneni, S. *Adv. Mater.* **2004**, *16*, 1629.
(57) Zhang, G.; Fang, H.; Yang, H.; Jauregui, L. a; Chen, Y. P.; Wu, Y. *Nano Lett.* **2012**, *12*, 3627.
(58) Fang, H.; Feng, T.; Yang, H.; Ruan, X.; Wu, Y. *Nano Lett.* **2013**, *13*, 2058.
(59) Zuo, P.; Zhang, S.; Jin, B. *J. Phys. Chem. C* **2008**, *112*, 14825.